



TITLE:

# Numerical Schemes for Solving the Burgers Equation (流体力学における非定常問題)

AUTHOR(S):

ALAM, MD.S.; KAWAMURA, TETUYA; KUWAHARA, KUNIO; TAKAMI, HIDEO

---

CITATION:

ALAM, MD.S. ...[et al]. Numerical Schemes for Solving the Burgers Equation (流体力学における非定常問題). 数理解析研究所講究録 1982, 449: 163-181

ISSUE DATE:

1982-02

URL:

<http://hdl.handle.net/2433/102934>

RIGHT:

Numerical schemes for solving the Burgers equation

by

Alam, Md. S., Kawamura, T.,  
Kuwahara, K. and Takami, H.

Department of Applied Physics  
Faculty of Engineering  
University of Tokyo

§1. Introduction

In this paper we discuss a number of numerical methods applied to solve the Burgers equation. This equation has the essential features of the Navier-Stokes equation, i.e., it contains both the advection and the diffusion terms. Therefore the Burgers equation serves as a touchstone of numerical methods for solving the Navier-Stokes equation.

In spite of many extensive investigations on Numerical solution of the Navier-Stokes equation, we still can not say definitely which method is most suitable and which result is most reliable, since we have very few exact solutions for flows of essentially nonlinear nature. On the contrary, exact analytical solutions are available in a number of cases for the Burgers equation. Therefore we can compare the numerical results with them and can examine the merits and demerits of various numerical methods.

In this paper we apply a number of numerical methods based on the finite-difference approximation and also the Fourier method to an initial- and boundary-value problem of Burgers equation. We compare the results with one another and with the exact solution, and discuss the merits of these numerical methods.

§2. Analytical solution

We shall consider the Burgers equation for  $u = u(x, t)$ :

$$\frac{\partial u}{\partial t} + u \frac{\partial u}{\partial x} = v \frac{\partial^2 u}{\partial x^2} \quad (0 < x < 1, \quad t > 0), \quad (2.1)$$

where  $v$  is a positive constant, under the initial and boundary conditions

$$u(x, 0) = \sin \pi x, \quad (2.2)$$

$$u(0, t) = 0, \quad u(1, t) = 0. \quad (2.3)$$

It is well known that this problem can be solved by the transformation

$$\psi(x, t) = \exp \left\{ \frac{1}{2v} \int^x u(\xi, t) d\xi \right\}. \quad (2.4)$$

In fact, eq. (2.1) is transformed into the diffusion equation

$$\frac{\partial \psi}{\partial t} = v \frac{\partial^2 \psi}{\partial x^2}, \quad (2.5)$$

the solution of which is given by

$$\psi(x, t) = \frac{1}{\sqrt{4\pi vt}} \int_{-\infty}^{\infty} \psi(\xi, 0) \exp \left\{ -\frac{(x-\xi)^2}{4vt} \right\} d\xi. \quad (2.6)$$

Therefore, we can get the solution of our problem (2.1)~(2.3) in the following explicit form:

$$\begin{aligned} u(x, t) &= \frac{2v}{\psi} \frac{\partial \psi}{\partial x} \\ &= -\frac{1}{t} \frac{\int_{-\infty}^{\infty} (x-\xi) \psi(\xi, 0) \exp \left\{ -(x-\xi)^2 / 4vt \right\} d\xi}{\int_{-\infty}^{\infty} \psi(\xi, 0) \exp \left\{ -(x-\xi)^2 / 4vt \right\} d\xi}. \end{aligned} \quad (2.7)$$

This solution is shown in Fig.1 for the values of  $t$  ranging from 0 to 1.0 and for  $v = 0.01$ . The numerical integration of eq. (2.7) has been performed by trapezoidal rule with  $\Delta x = 1/40$ . Initial sinusoidal profile of  $u$  is deformed both by advection and by diffusion. With this exact solution we shall compare our results

obtained by means of various numerical methods based on finite-difference approximation and by the Fourier method.

### §3. Finite-difference and Fourier methods

We shall discuss here a number of finite-difference methods and the Fourier method used for solving our problem stated above (also see Table 1).

Explicit method E-1 Equation (2.1) is discretized by use of forward difference in  $t$  and centered difference in  $x$ .

Explicit method E-2 The same as in E-1, but after rewriting the advection term  $u \partial u / \partial x$  in conservation form  $\partial (u^2/2) / \partial x$ .

Explicit method E-3 MacCormack's scheme<sup>1)</sup> for eq.(2.1). Formal order of accuracy is higher than those of E-1 and E-2.

Explicit method E-4 The same as above, but for the equation of conservation form.

Implicit method I-1 Standard Crank-Nicolson's scheme for eq.(2.1).

Implicit method I-2 The same as above, but for the equation of conservation form.

Characteristic method C-1 First determine the  $x$ -coordinate  $\xi_j^n$  of the point of intersection of the line  $t = n\Delta t$  and the characteristic line issuing backward from mesh point  $(j\Delta x, (n+1)\Delta t)$ , the direction of which is tentatively given by the value of  $u$  at the mesh point  $(j\Delta x, n\Delta t)$  (see Fig.2). Then, by use of the interpolated values of  $u$  at points  $(\xi_j^n, n\Delta t)$ , integrate along the characteristic line the equation

$$\frac{Du}{Dt} = v \frac{\partial^2 u}{\partial x^2} \quad (3.1)$$

according to Crank-Nicolson's implicit scheme. In order to determine the final values of  $u$  at the mesh points on the line

$t = (n+1)\Delta t$ , iterative procedure is necessary, in which the values of  $u$  as well as the directions of the characteristic lines are improved until they converge.

Characteristic method C-2 The essential idea is the same as in C-1, but we first determine the  $x$ -coordinates  $\xi_j^{n+1}$  of the points of intersection of the line  $t = (n+1)\Delta t$  and the characteristic lines issuing from the mesh points on the line  $t = n\Delta t$  (see Fig.3), and then integrate eq.(3.1) according to Crank-Nicolson's scheme to determine the values of  $u$  at these points. The values of  $u_j^{n+1}$  are computed in terms of them by interpolation. Furthermore, we use mesh points spaced nonuniformly in the  $x$ -direction, i.e., we take the coordinate of the  $n$ th grid point as  $\sqrt{n/N}$  instead of  $n/N$  in C-1, where  $N$  is the total number of mesh intervals. On the other hand, time interval  $\Delta t$  is fixed to be constant.

Characteristic method C-3 We use spatial mesh spacing which is variable in time. Initial spacing of the mesh points is uniform. The mesh points on the line  $t = (n+1)\Delta t$  are determined as its intersections with the characteristic line issuing from the mesh points on  $t = n\Delta t$  (see Fig.4). The time interval  $\Delta t$  is fixed.

Fourier method We expand the solution in a Fourier series as

$$u(x,t) = \sum_{n=1}^{\infty} u_n(t) \sin n\pi x, \quad (3.2)$$

and substitute it into eq.(2.1). If we assume that all the Fourier coefficients except  $u_1(t), u_2(t), \dots, u_N(t)$  to be zero, we get a system of ordinary differential equations for  $u_n(t)$ :

$$\frac{du_n}{dt} = \frac{\pi}{2} \left( n \sum_{k=n+1}^N u_k u_{k-n} - \sum_{k=1}^{n-1} k u_{n-k} u_k \right) - \nu \pi^2 n^2 u_n$$

$$(n = 1, 2, \dots, N). \quad (3.3)$$

These equations are to be solved numerically by the Runge-Kutta

method.

#### §4. Numerical results and discussion

We have fixed the value  $\nu = 0.01$  throughout. We shall show and discuss the results of computation performed with the parameters  $\Delta x = 1/40$  ( $N = 40$  in the Fourier method) and  $\Delta t = 1/80$ . This pair of values guarantees stability in the framework of the linear theory\*. The summary of the computation performed with various values of the parameters is given in Table 2.

Figures 5 and 6 show the profiles of  $u$  computed by the methods E-1 and E-2 respectively. We find some damping a little more than that in the exact solution. It is clear that the result by E-2 is better than that by E-1.

Application of E-3 gives better result as is expected from the order of accuracy of this scheme (Fig.7). However, there appears a sharp peak on the profile near the boundary  $x = 1$ . On the other hand, the method E-4 gives a smooth profile which agrees well with the exact solution (Fig.8).

---

\*The stability criterion for the linear difference equation

$$u_j^{n+1} = u_j^n - \frac{a}{2} \frac{\Delta t}{\Delta x} (u_{j+1}^n - u_{j-1}^n) + \nu \frac{\Delta t}{(\Delta x)^2} (u_{j+1}^n - 2u_j^n + u_{j-1}^n) \quad (4.1)$$

is<sup>2)</sup>

$$\nu \frac{\Delta t}{(\Delta x)^2} \leq \frac{1}{2} \quad \text{and} \quad \nu \geq \frac{1}{2} a^2 \Delta t. \quad (4.2)$$

In our case, the critical value for  $\Delta t$  is

$$(\Delta t)_c = \min\left(\frac{1}{32}, \frac{1}{50}\right) = \frac{1}{50}. \quad (4.3)$$

Here the constant  $a$  is put to be equal to 1, since  $0 \leq u \leq 1$  in our problem

It should be noted that the value of  $\Delta t$  exceeding the critical value  $(\Delta t)_c$  given by the linear stability theory does not necessarily give rise to exponential growth of the modes of large wave numbers. Fig.9 shows this point. Such growth does not appear when we apply the method E-1 even with  $\Delta t = 1/40$  ( $> (\Delta t)_c$ ). Very fast damping has occurred instead.

Fig.10 shows the result obtained by the method I-1. Over-shooting occurs also in this case. The result is much improved by I-2 (Fig.11).

Now in characteristic methods, the effect of advection and diffusion is taken into account separately, and each effect is computed according to a scheme suitable for expressing respective physical mechanism. In fact, the results computed by C-1 (Fig.12), C-2 (Fig.13) and C-3 (Fig.14) are good.

Fig.15 shows the result obtained by the Fourier method. The Fourier series (3.2) has been truncated at the 40th term, i.e., we have taken  $N = 40$ . This is in a sense equivalent to taking  $\Delta x = 1/40$  in finite-difference methods. The result is fairly good except the occurrence of wavy pattern superposed on otherwise smooth profile.

Computation with  $N = 16$  and  $\Delta t = 1/10$  has revealed an interesting phenomenon. As Fig.16 shows, oscillation appears at about  $t = 0.4$ , and its growth seems to invalidate the numerical solution. After some time, however, the oscillation begins to die out until a realistic pattern is recovered. Examination of the behavior of each Fourier component makes this change of pattern clearer. We have shown this in Fig.17.

Lastly, in order to see the accuracy of the results in more detail, we have shown in Fig.18 the relative errors of the numerical solutions, which is defined by

$$e_r = \frac{u_a - u}{u}, \quad (4.4)$$

where  $u$  and  $u_a$  denote the values of the exact and approximate solutions respectively.

## §5. Conclusion

From the numerical computation shown above, we conclude the following.

The results obtained by E-2, E-4 and I-2 are better than those by E-1, E-3 and I-1 respectively. This fact suggests that, if we use finite-difference method and if the formal order of accuracy is the same, we should adopt the schemes based on the equation written in conservation form.

By comparison of the relative errors (Fig.18) we can say that the characteristic methods are superior to the conventional finite-difference methods. The method C-2 is found to be the best in view of its high accuracy and not very large amount of computing time. For general purpose, however, the method C-3 should be regarded as preferable, since the position of, say, shock formation is not known beforehand in general problems. In fact, changing the mesh spacing is automatically done in C-3, in such a way that we have finer spacing for steeper portion of  $u$ -profile. On the other hand, difficulty will arise when one applies C-3 to two- or three-dimensional problem, because in this case the mesh spanned by variable mesh points will become strained in a complicated way so that determination of their new positions by interpolation require large amount of computing time. This is the most important point that must be overcome in attacking multi-dimensional problems by means of the method C-3.

On the other hand, Fourier method shows high accuracy for  $u$  (see Fig.18 (h)), although the accuracy must be low for its space derivatives. The greatest advantage of this method must be that we can see the time change of each component separately and therefore can estimate the effect of nonlinear coupling between different modes to some extent. By Fourier method,



however, we can not examine the detailed behavior of the solution locally if the number of components is fixed, as by taking non-uniform mesh in finite-difference methods. Also we have rather large amount of computing time to ensure high accuracy as shown in Table 2.

In conclusion we can say that, in this example C-2 or C-3 is best of all the methods tested in this paper. Also we have found that large values of  $\Delta t$  violating the linear stability condition do not necessarily lead to such exponential growth of the solution that is inevitable in linear problems. This fact suggests that one must be careful enough in interpreting the seemingly realistic results of numerical simulation of nonlinear phenomena.

#### References

- 1) MacCormack, R. W. and Lomax, H.: Numerical solution of compressible viscous flows. Ann. Rev. Fluid Mech. 11 (1979) 289-316.
- 2) Hirt, C. W.: Heuristic stability theory for finite-difference equations. J. comput. Phys. 2 (1968) 339-355.

Table 1.

Some of the finite-difference schemes used in this paper,  $u_j^n$  being finite-difference approximant to  $u(j\Delta x, n\Delta t)$ .

Method E-1

$$u_j^{n+1} = u_j^n - \frac{1}{2} \frac{\Delta t}{\Delta x} u_j^n (u_{j+1}^n - u_{j-1}^n) + v \frac{\Delta t}{(\Delta x)^2} (u_{j+1}^n - 2u_j^n + u_{j-1}^n).$$

Method E-2

$$u_j^{n+1} = u_j^n - \frac{1}{4} \frac{\Delta t}{\Delta x} \{(u_{j+1}^n)^2 - (u_{j-1}^n)^2\} + v \frac{\Delta t}{(\Delta x)^2} (u_{j+1}^n - 2u_j^n + u_{j-1}^n).$$

Method E-3

predicted values:

$$\tilde{u}_j^{n+1} = u_j^n - \frac{\Delta t}{\Delta x} u_j^n (u_j^n - u_{j-1}^n) + v \frac{\Delta t}{(\Delta x)^2} (u_{j+1}^n - 2u_j^n + u_{j-1}^n).$$

corrected values:

$$\begin{aligned} u_j^{n+1} = \frac{1}{2} (u_j^n + \tilde{u}_j^{n+1}) - \frac{1}{2} \frac{\Delta t}{\Delta x} \tilde{u}_j^{n+1} (\tilde{u}_{j+1}^{n+1} - \tilde{u}_j^{n+1}) \\ + \frac{v}{2} \frac{\Delta t}{(\Delta x)^2} (\tilde{u}_{j+1}^{n+1} - 2\tilde{u}_j^{n+1} + \tilde{u}_{j-1}^{n+1}). \end{aligned}$$

Method E-4

predicted values:

$$\tilde{u}_j^{n+1} = u_j^n - \frac{1}{2} \frac{\Delta t}{\Delta x} \{(u_j^n)^2 - (u_{j-1}^n)^2\} + v \frac{\Delta t}{(\Delta x)^2} (u_{j+1}^n - 2u_j^n + u_{j-1}^n).$$

corrected values:

$$\begin{aligned} u_j^{n+1} = \frac{1}{2} (u_j^n + \tilde{u}_j^{n+1}) - \frac{1}{4} \frac{\Delta t}{\Delta x} \{(\tilde{u}_{j+1}^{n+1})^2 - (\tilde{u}_j^{n+1})^2\} \\ + \frac{v}{2} \frac{\Delta t}{(\Delta x)^2} (\tilde{u}_{j+1}^{n+1} - 2\tilde{u}_j^{n+1} + \tilde{u}_{j-1}^{n+1}). \end{aligned}$$

Method I-1

$$\begin{aligned}
u_j^{(p+1)} = & \{ u_j^n - \frac{1}{8} \frac{\Delta t}{\Delta x} (u_j^n + u_j^{(p+1)}) (u_{j+1}^n - u_{j-1}^n) + \frac{\nu}{2} \frac{\Delta t}{(\Delta x)^2} (u_{j+1}^{(p)} + u_{j-1}^{(p+1)}) \\
& + \frac{\nu}{2} \frac{\Delta t}{(\Delta x)^2} (u_{j+1}^n - 2u_j^n + u_{j-1}^n) \} / (1 + \nu \frac{\Delta t}{(\Delta x)^2}).
\end{aligned}$$

(p) and (p+1) attached to the top of  $u_j^{n+1}$  etc. designate the numbers of iteration.

Method I-2 (conservation form)

$$\begin{aligned}
u_j^{(p+1)} = & \{ u_j^n - \frac{1}{8} \frac{\Delta t}{\Delta x} (u_{j+1}^n)^2 - (u_{j-1}^n)^2 + (u_{j+1}^{(p)})^2 - (u_{j-1}^{(p+1)})^2 + \frac{\nu}{2} \frac{\Delta t}{(\Delta x)^2} (u_{j+1}^{(p)} + u_{j-1}^{(p+1)}) \\
& + \frac{\nu}{2} \frac{\Delta t}{(\Delta x)^2} (u_{j+1}^n - 2u_j^n + u_{j-1}^n) \} / (1 + \nu \frac{\Delta t}{(\Delta x)^2}).
\end{aligned}$$

Table 2. Summary of the numerical results

computational scheme	$\Delta t$	$ e_r  = \left  \frac{u - u_a}{u} \right $	CPU time up to $t=1.0$	stability condition (linear theory)
Method E-1	1/10	diverging	-	$t \leq \frac{1}{50}$
	1/20	diverging	-	
	1/40	very large	0.560 s	
	1/80	very large	0.566	
Method E-2	1/10	diverging	-	
	1/20	diverging	-	
	1/40	very large	0.545	
	1/80	very large	0.560	
Method E-3	1/10	diverging	-	$\Delta t \leq 0.02254 \approx 1/44$ $\Delta t \leq 0.0313 \approx 1/32$ (numerical)
	1/20	diverging	-	
	1/40	30.9 %	0.560	
	1/80	28.6	0.577	
Method E-4	1/10	diverging	-	$\Delta t \leq 0.0350 \approx 1/29$ (numerical)
	1/20	diverging	-	
	1/40	9.7	0.540	
	1/80	7.6	0.545	
Method I-1	1/10	50.1	0.560	stable for all $\Delta t$
	1/20	43.6	0.580	
	1/40	42.5	0.605	
	1/80	42.2	0.621	
Method I-2	1/10	13.9	0.546	stable for all $\Delta t$
	1/20	9.4	0.559	
	1/40	8.1	0.561	
	1/80	7.8	0.590	
Method C-1	1/10	24.9	1.920	stable for all $\Delta t$
	1/20	15.5	2.250	
	1/40	10.0	3.300	
	1/80	4.7	4.920	
Method C-2	1/10	diverging	-	
	1/20	diverging	-	
	1/40	3.7	0.732	
	1/80	1.7	0.794	
Method C-3	1/10	diverging	-	
	1/20	diverging	-	
	1/40	38.54	1.025	
	1/80	37.55	1.605	
Fourier Method	1/10	diverging	-	$\Delta t \leq 0.012665 \approx 1/78.96$ (for diffusion equation)
	1/20	diverging	-	
	1/40	diverging	-	
	1/80	1.2	2.134	

$$\nu = 0.01$$

$$\Delta x = 1/40 \quad (\text{finite-difference method})$$

$$N = 40 \quad (\text{Fourier method})$$

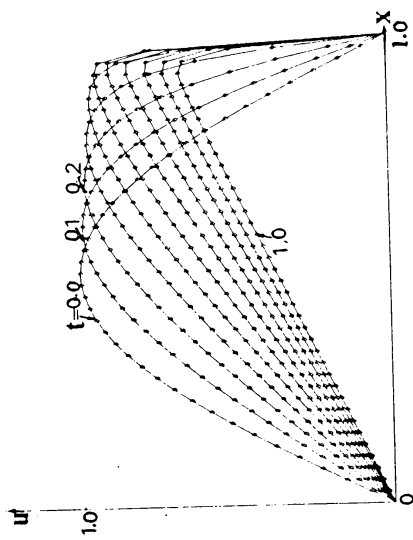


Fig.1. Exact solution.

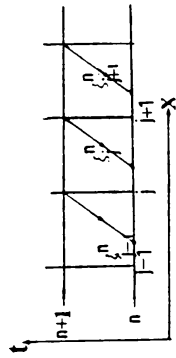


Fig.2. Computational scheme of Method C-1.

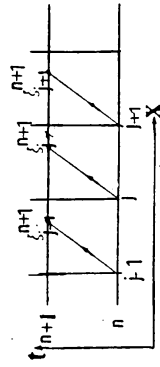


Fig.3. Computational scheme of Method C-2.

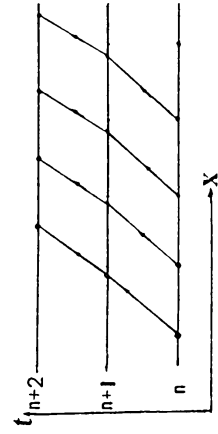


Fig.4. Computational scheme of Method C-3.

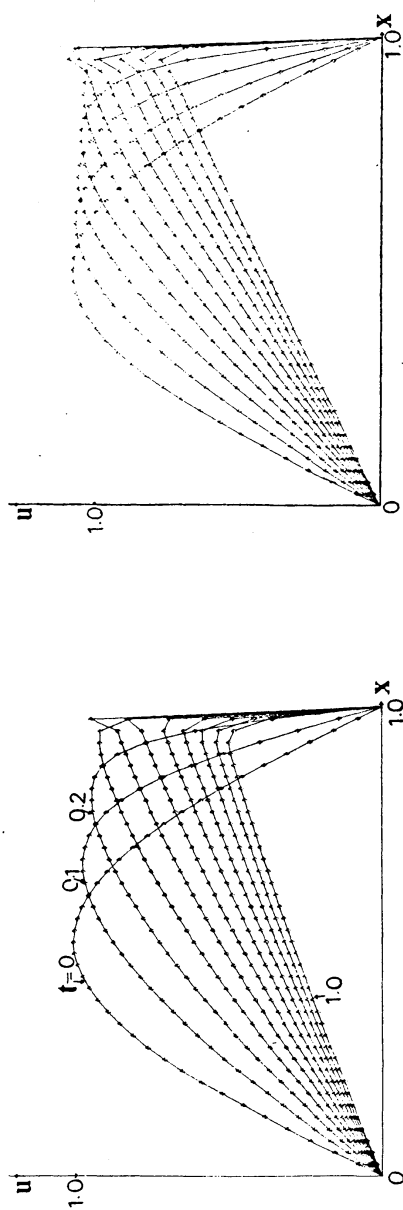


Fig. 5. Method E-1;  $\Delta x = 1/40$ ,  $\Delta t = 1/80$ .

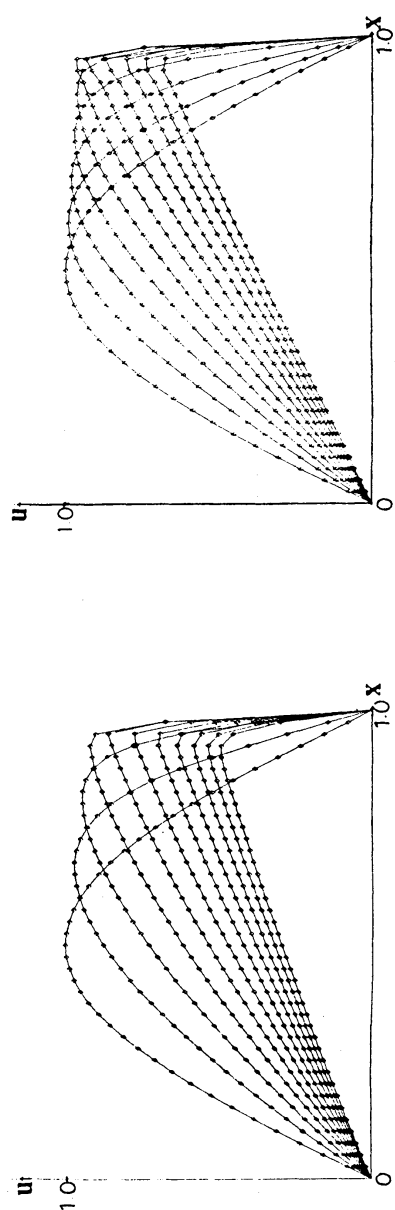


Fig. 6. Method E-2;  $\Delta x = 1/40$ ,  $\Delta t = 1/80$ .

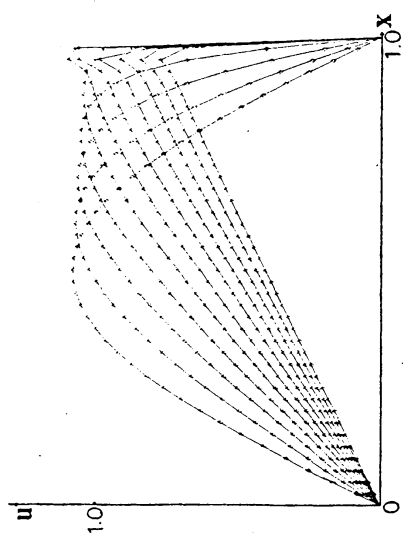


Fig. 7. Method E-3;  $\Delta x = 1/40$ ,  $\Delta t = 1/80$ .

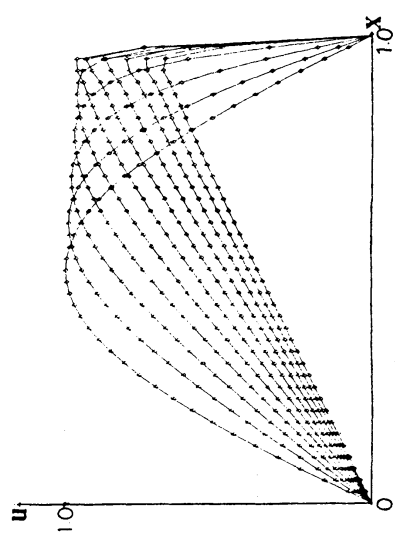
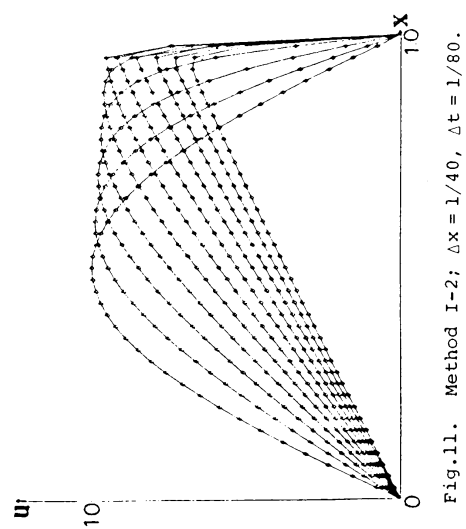
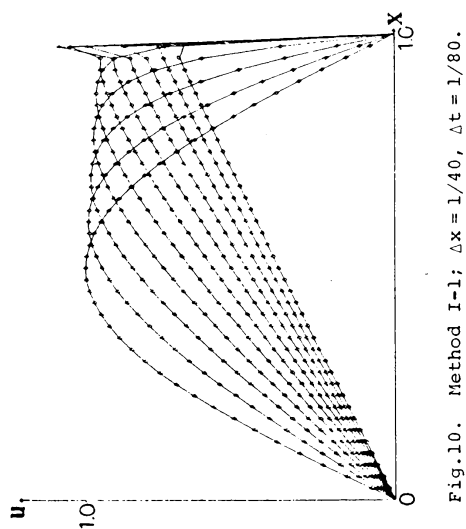
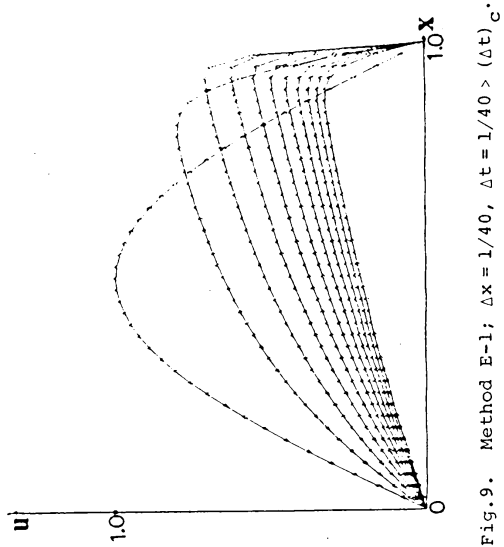


Fig. 8. Method E-4;  $\Delta x = 1/40$ ,  $\Delta t = 1/80$ .



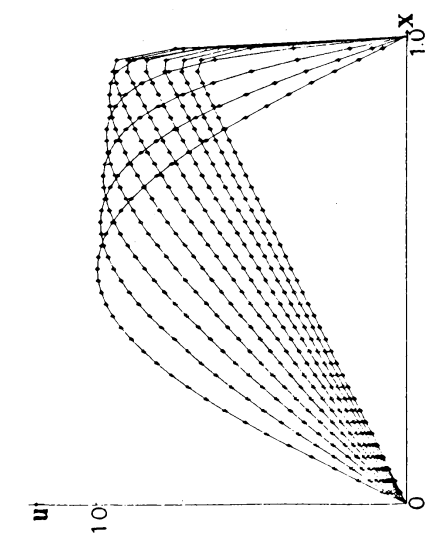


Fig.12. Method C-1;  $\Delta x = 1/40$ ,  $\Delta t = 1/80$ .

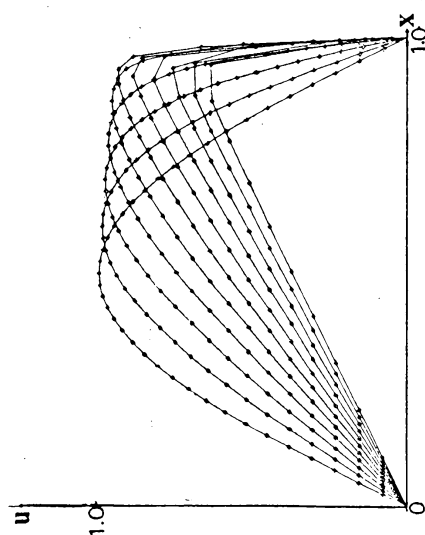


Fig.14  
Method C-3; mesh spacing variable and nonuniform,  
 $\Delta t = 1/80$ .

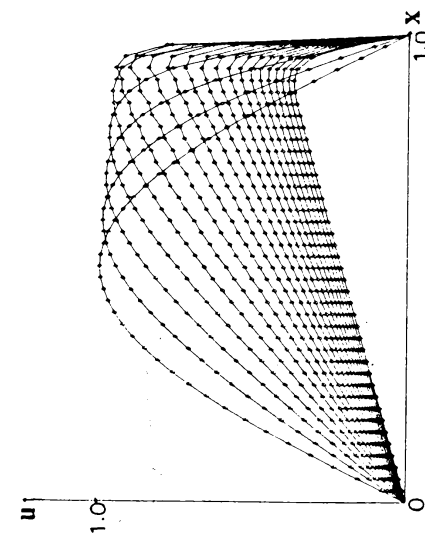


Fig.15. Fourier method;  $N = 40$ ,  $\Delta t = 1/80$ .

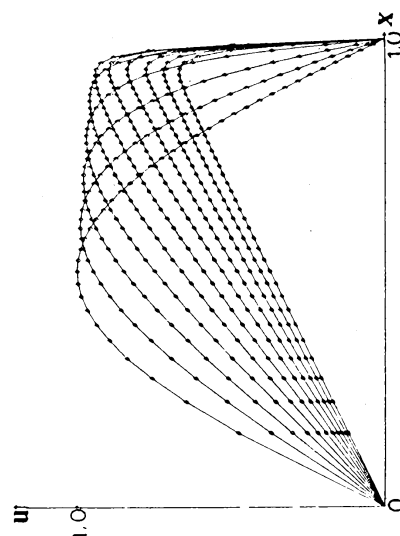


Fig.13  
Method C-2; mesh spacing not uniform,  $\Delta t = 1/80$ .

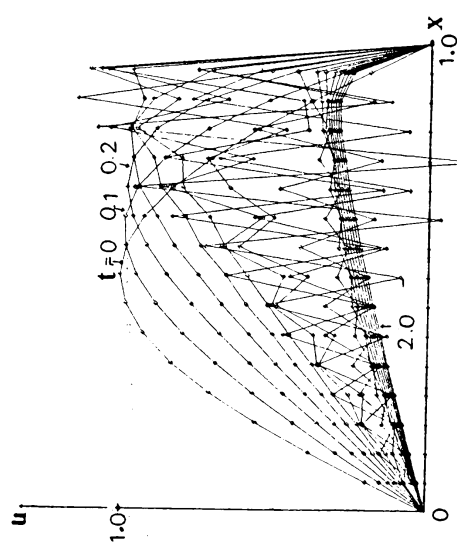


Fig.16. Fourier method;  $N = 16$ ,  $\Delta t = 1/10$ .



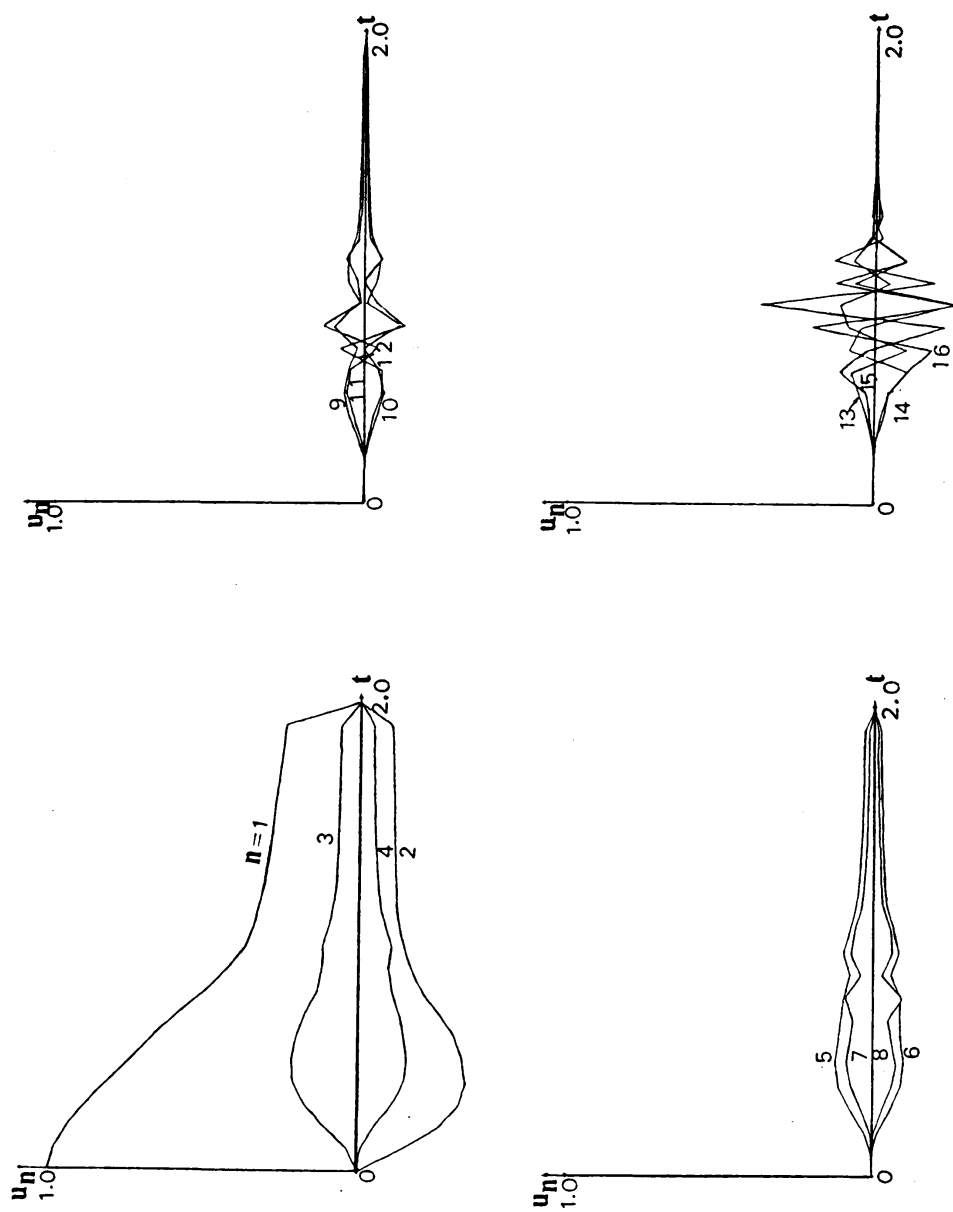


Fig.17. Behavior of the Fourier components for the case shown in Fig.16.

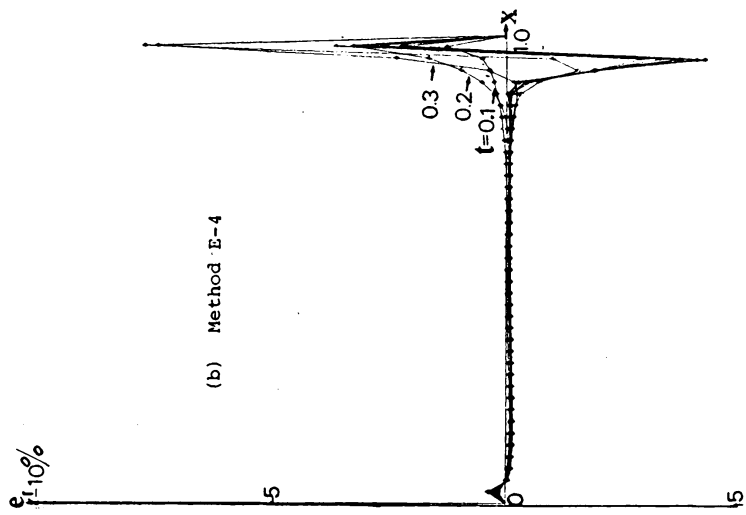
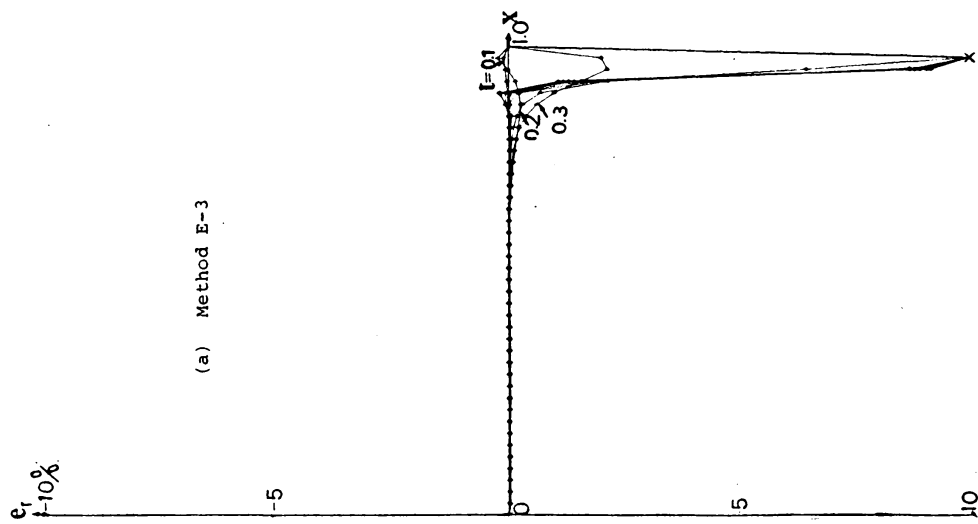


Fig. 18. Relative errors;  $\Delta x = 1/40$ ,  $\Delta t = 1/80$ .

